Electronic Supplementary Material (ESI) for Journal of Materials Chemistry A.


Supplementary Information for

# Oxygen loss and surface degradation during electrochemical cycling of lithium-ion battery cathode material $LiMn_2O_4$

Xiang Gao,[a,†] Yumi H. Ikuhara,[a] Craig A. J. Fisher,[*,a] Rong Huang,[b] Akihide Kuwabara,[a] Hiroki Moriwake,[a] Keiichi Kohama[c] and Yuichi Ikuhara[*,a,d]

[a]Nanostructures Research Laboratory, Japan Fine Ceramics Center, Nagoya 456-8587, Japan
[b]Key Laboratory of Polar Materials and Devices, East China Normal University, Shanghai 200062, China
[c]Battery Materials Division, Toyota Motor Corporation, Susono, Shizuoka 410-1193, Japan
[d]Institute of Engineering Innovation, The University of Tokyo, Tokyo 113-8656, Japan

[†] Now at Center for High Pressure Science and Technology Advanced Research (HPSTAR), Beijing 100094, China
*Email -c_fisher@jfcc.or.jp

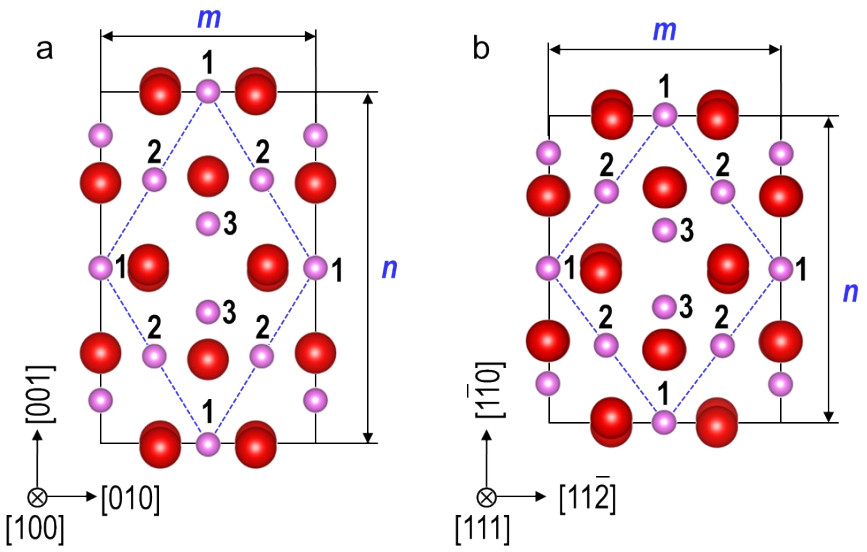


**Figure S1.** Projections of the tetragonal $Mn_3O_4$ (space group $I4_1/amd$) unit cell along (a) [100] and (b) [111] directions showing three types of Mn sites, labelled 1, 2 and 3. Mn1 and Mn2 columns contain only $Mn^{3+}$ atoms sitting on octahedral positions. They form a diamond configuration but have different atom densities (Mn1 columns having twice the atom density of Mn2 columns) similar to the case for λ-$MnO_2$ (Fig. 1). Mn3 columns are composed entirely of $Mn^{2+}$ ions on tetrahedral sites. The ratios between projected distances of the short (*m*) and long (*n*) Mn-diamond diagonals are 0.610 and 0.924 when viewed along [100]=[010] and [111] directions, respectively.

**Analysis of Li-deficient surface layer**

Measurements from the HAADF image in Figure 2b of the main manuscript give an *m*:*n* ratio of 0.67±0.02 for the surface region when normalised to that of the bulk structure (which is assumed to have a cubic λ-$MnO_2$ structure with $m:n = \frac{\sqrt{2}}{2}$. The results indicate that surficial $Mn_3O_4$ is oriented with the [100] (equivalent to [010]) direction parallel to the [110] direction of $LiMn_2O_4$; presumably this results in a smaller lattice strain compared to a [111] orientation with its significantly larger *m*:*n* ratio. The slightly larger measured ratio of 0.67±0.02 compared to that of single crystal $Mn_3O_4$ (0.610) suggests the surface also contains a reasonably high concentration of defects, probably Mn vacancies, while also being constrained by the lithium manganese film underneath (lattice strain). Note that the error values are standard deviations taken from no less than eight sets of data.

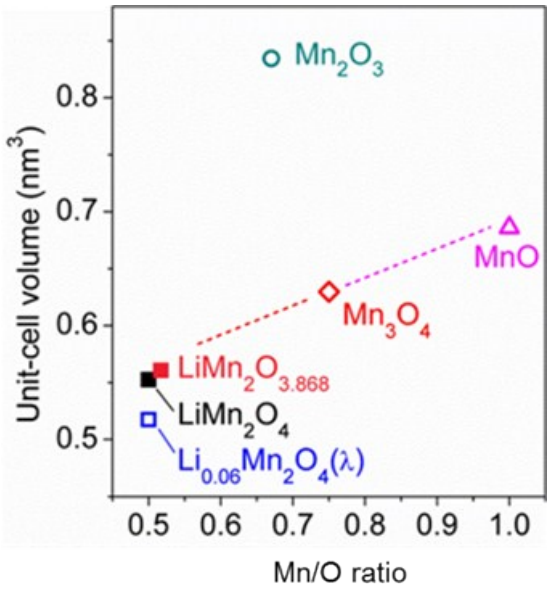


**Figure S2.** Comparison of unit-cell volumes of various (lithium) manganese oxides (after conversion to pseudo-cubic unit cells where necessary). Lattice parameters for $LiMn_2O_4$, $Li_{0.06}Mn_2O_4$ and $LiMn_2O_{3.868}$ were taken from ref. S1, and those for $Mn_3O_4$, MnO and $Mn_2O_3$ were taken from refs. S2, S3 and S4, respectively.

**Thin film deposition and microscopy techniques**

*Thin film deposition*

Au films were deposited on $Al_2O_3$ (0001) single crystals by rf-diode sputtering for use as substrates. The target was a 99.99% Au plate that covered the cathode. Before sputtering, each $Al_2O_3$ (0001) substrate was chemically cleaned and set on a table that covered the anode. The chamber was evacuated to a pressure of $3\times10^{-4}$ Pa and backfilled with 99.999% pure argon gas. The argon gas pressure was kept constant at 1.5 Pa throughout deposition. The substrate temperature was held at 650°C, and the sputtering power was set at 100 W.

$LiOCH(CH_3)_2$ and $Mn(OC_3H_7)_2$ were used as starting metalorganic precursors with 2-ethoxyethanol ($C_2H_5OC_2H_4OH$; EGMEE) as the solvent. The precursors were dissolved in EGMEE under dry $N_2$ atmosphere and refluxed at 135°C for 3 h to produce $LiOC_2H_4OC_2H_5$ and $Mn(OC_2H_4OC_2H_5)_4$ by complete reaction. After cooling to room temperature, these two solutions were condensed in a rotary evaporator and added to fresh EGMEE solution to remove the $(CH_3)_2CHOH$ byproduct. A homogeneous metalorganic [Li–Mn–O] precursor solution was prepared by mixing these two solutions and refluxing at 135°C for 1 h.

The $LiMn_2O_4$ precursor films were fabricated from the brown [Li–Mn–O] metalorganic precursor solution by spin coating onto clean $Au/Al_2O_3(0001)$ substrates at a spinning speed of 2000 rpm for 20 s under flowing $N_2$ gas. Precursor films were then transferred to a single-zone tube furnace and heated at 200°C for 30 min to remove the organic ligands. This was followed by further heating to 750°C at a rate of 5 °C/min and annealing for 1 h in oxygen. To obtain thicknesses of around 100 nm, this procedure was repeated several times.

*TEM specimen preparation and STEM measurements*

Pristine and cycled thin film samples were coated with a protective layer of amorphous carbon (> 50 nm). Surfaces of each sample were cleaned prior to coating using dimethyl carbonate (DMC) in argon atmosphere in a glove box and the samples delivered within sealed storage bags filled with high-purity argon. Cross-sectional specimens for STEM observations were prepared by dual-beam focused ion beam scanning microscopy (NB5000, Hitachi, Japan) using a Ga-ion accelerating voltage ranging from 40 to 2 kV, followed by ion milling (Gatan 691, Gatan, USA) at accelerating voltages of 1.5 to 0.2 kV while cooling with liquid nitrogen. Milled samples underwent argon plasma cleaning (Solarus 950, Gatan, USA) to remove almost completely any residual surface contamination.A 200 kV JEM-ARM (JEOL Ltd.) microscope equipped with a spherical-aberration corrector (CEOS GmbH) enabling structures to be probed with sub-angstrom resolution was utilised for STEM imaging. A convergence angle of 25 mrad and annular dark-field detector inner/outer angles of 70/240 mrad were chosen for HAADF imaging.

STEM-EELS analysis was carried out using a JEM-ARM200F (JEOL Ltd.) microscope equipped with a spherical-aberration corrector (CEOS GmbH), a Gatan Image Filter and a Wien-filter type monochromator. The microscope was installed in a room designed and constructed to minimise AC magnetic fields, floor vibrations, air flow disturbances, and temperature and acoustic fluctuations to provide the optimum environment for STEM analysis. An accelerating voltage of 120 kV, convergence angle of 36 mrad, and energy resolution of 0.3 eV (determined by measuring the full-width half-maximum (FWHM) of the zero-loss speak) were selected for analysis of all edges. Electron energy-loss spectra were recorded in scanning (STEM) mode under the following conditions: a dispersion of 0.1 eV/channel for all edges and integration time of 0.2 s per

read-out for the Li-*K* and Mn-$M_{2,3}$ edges, and of 1.0 s per read-out for the O-*K* and Mn-$L_{2,3}$ edges. All spectra were taken from thin specimen regions. Quantitative analysis of the Mn valence state was carried out using the white-line ratio method.[S5,S6]

To protect the film surface from possible specimen damage during FIB milling, samples were coated with a comparatively thick amorphous carbon layer (no less than 50 nm). Additionally, a thick slice was prepared to ensure a sufficiently well-protected region inside the specimen, as damage at the edges is unavoidable. To further reduce the amount of surface damage, the top layer was removed by gentle (low-voltage) ion-milling at low temperature. Finally, Ar plasma cleaning was used to remove any remaining surface contamination.

To minimise possible electron beam irradiation effects, all images and spectra were acquired without pre-beam irradiation; in addition, a relatively low voltage of 120 kV, a low probe current of 11 pA (using a small monochromator slit size of 1 μm) and a short well time (≤ 20 μs) with fast scanning rate (dwell time ≤ 2 μs) over a relatively large specimen area were used for imaging and spectroscopy analysis, respectively.

## References


[S1] M. Yonemura, A. Yamada, H. Kobayashi, M. Tabuchi, T. Kamiyama, Y. Kawamoto and R. Kanno, *J. Mater. Chem.* 2004, **14**, 1948–1958.
[S2] B. Boucher, R. Buhl and M. Perrin, *J. Phys. Chem. Solids* 1971, **32**, 2429–2437.
[S3] J. Zhang, *Phys. Chem. Miner.* 1999, **26**, 644–648.
[S4] S. Geller, *Acta Crystallogr. Sect. B* 1971, **27**, 821–828.
[S5] M. Varela, M. P. Oxley, W. Luo, J. Tao, M. Watanabe, A. R. Lupini, S. T. Pantelides, and S. J. Pennycook, *Phys. Rev. B* 2009, **79**, 085117.
[S6] X. Gao, Y. H. Ikuhara, C. A. J. Fisher, H. Moriwake, A. Kuwabara, H. Oki, K. Kohama, R. Yoshida, R. Huang and Y. Ikuhara, *Adv. Mater. Interfaces* 2014, **1**, 1400143.